A compensation technique for accurate acceleration measurements using a UAV-deployable and retrievable sensor package

Joud Satme; Department of Mechanical Engineering
Corinne Smith; Department of Mechanical Engineering
Austin R.J. Downey; Department of Mechanical, Civil and Environmental Engineering
Jason D. Bakos; Department of Computer Science and Engineering
Nikolaos Vitzilaios; Department of Mechanical Engineering
Dimitris Rizos; Department of Civil and Environmental Engineering

UNIVERSITY OF SOUTH CAROLINA

Outline

- Methodology:
  - Sensor package breakdown
    - Features
    - Hardware
    - Algorithm
  - Deployment and retrieval
  - Transfer function-based filter
    - Approach and assumptions
    - Model training
- Experimentation:
  - Bench-top testing (Training)
  - Structure testing (Validation)
- Results and Discussion:
  - Experimental outcomes
  - Findings and limitations
- Future work:
  - Sensor improvement
  - Edge implementation

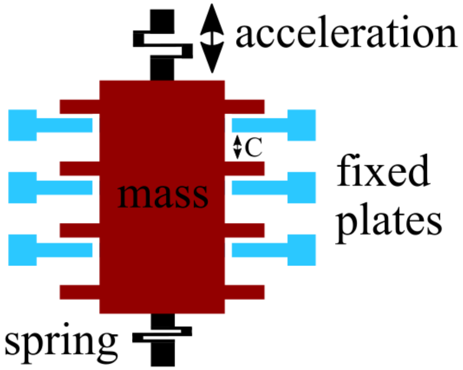

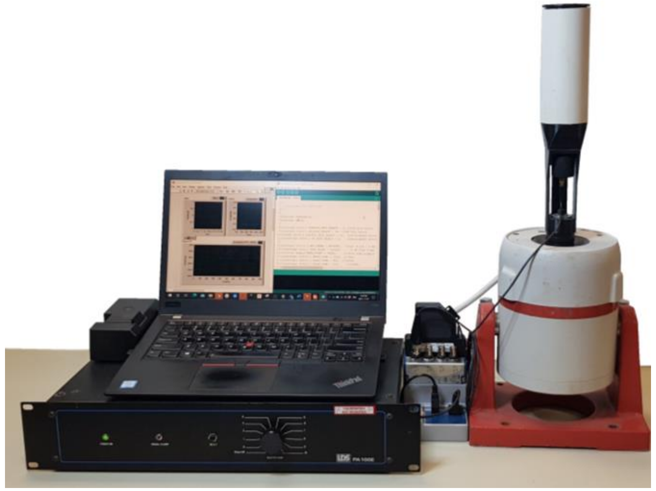

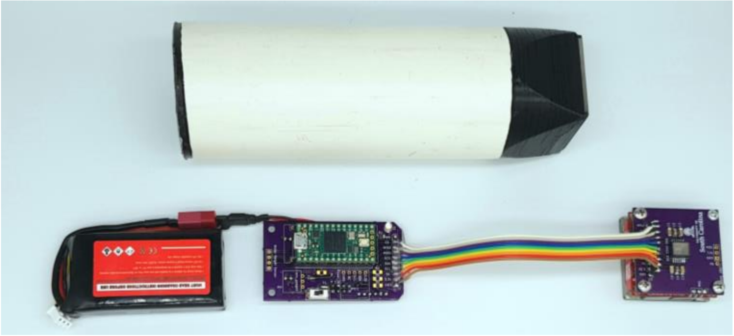

Introduction

- Importance of structural health monitoring.
- Current systems in use and their features.
- Problem statement:
    - Long-term data collection.
    - Rapid large-scale deployment.
    - Transmissibility losses.
- Proposed approach:
    - Stand-alone sensor package.
    - UAV-delivery system.
    - Transfer function-based compensation method.

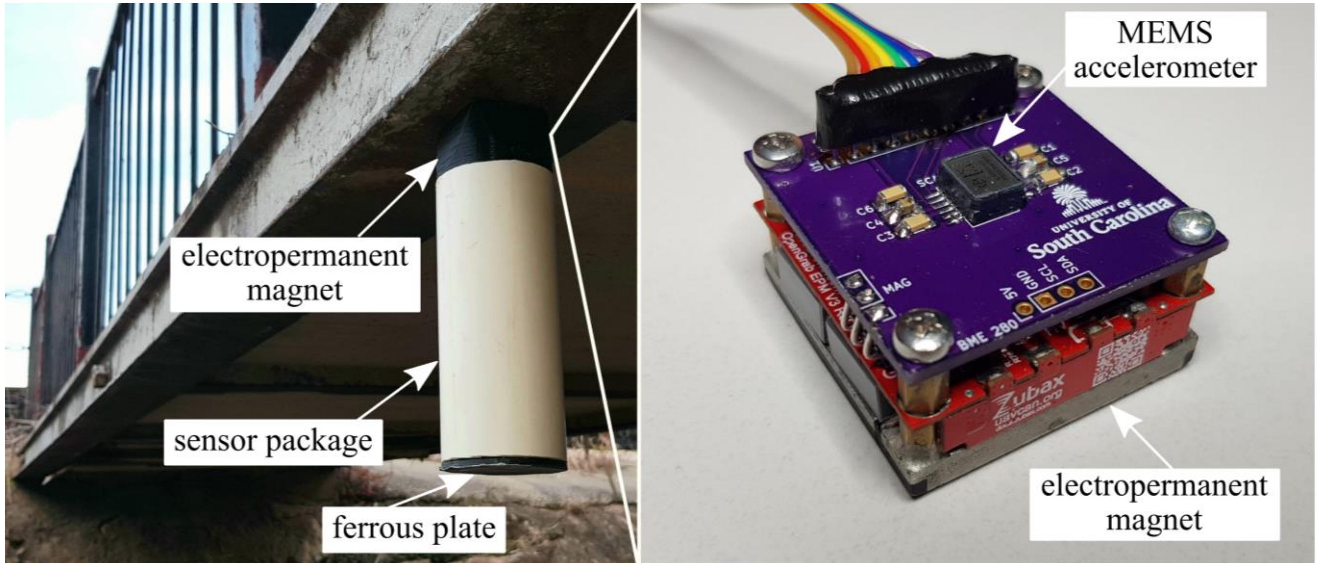

Sensor package breakdown

- Features:
  - UAV deployable sensor package designed with high mobility in mind.
  - Power and memory storage subsystems in anticipation of long-term deployment.
  - Wireless subsystem for data transmission and IO commands.
  - Docking subsystem utilizing electropermanent magnets.
  - Frame of the package designed with minimizing transmissibility losses in mind.
  - Maximum sampling rate 28 S/s.

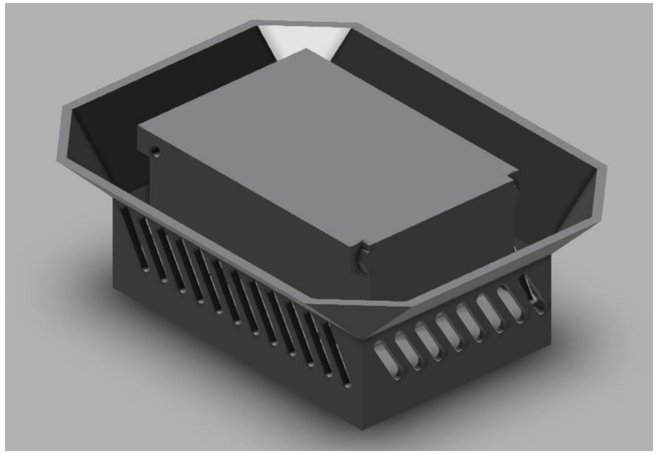

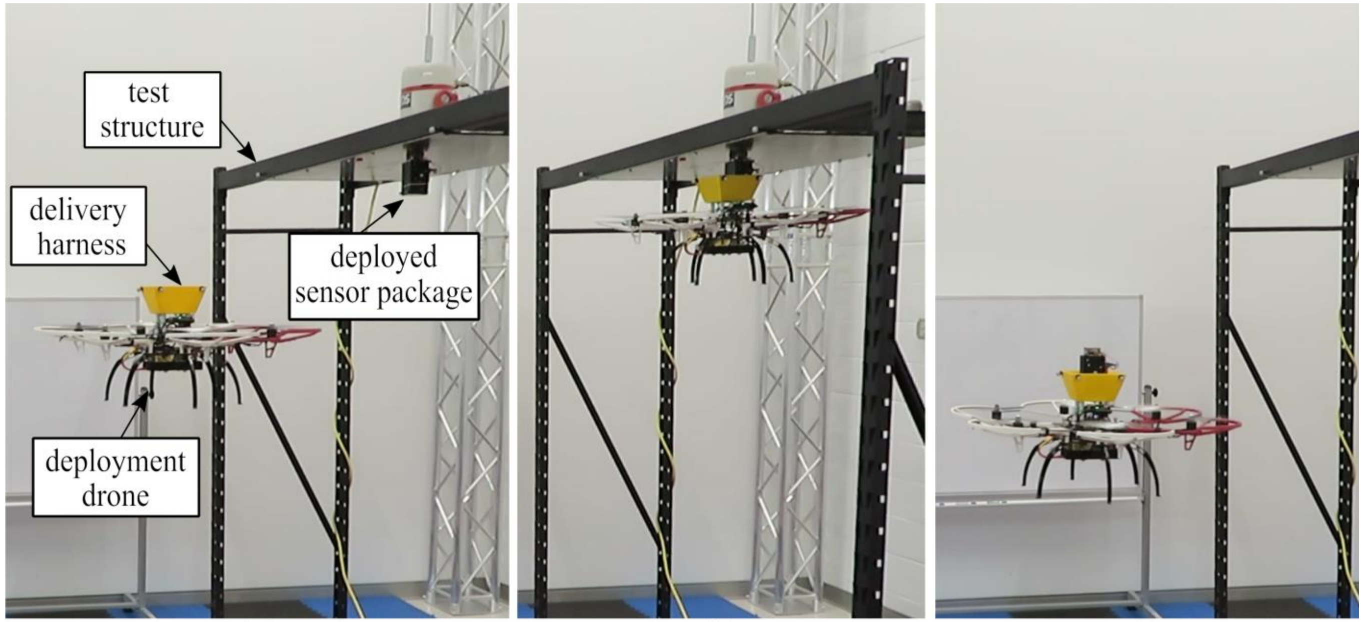

Sensor package breakdown

- Hardware:
  - Processor: ARM Cortex-M7 on Teensy 4.0 microcontroller.
  - SCA3300-d01 MEMS accelerometer.
  - EPM V3R5C electropermanent magnet.
  - Nonvolatile memory (SD card) for long-term storage.
  - Lithium polymer battery, voltage regulation and monitoring.
  - NRF24L01 Nordic Semiconductor wireless transceiver.

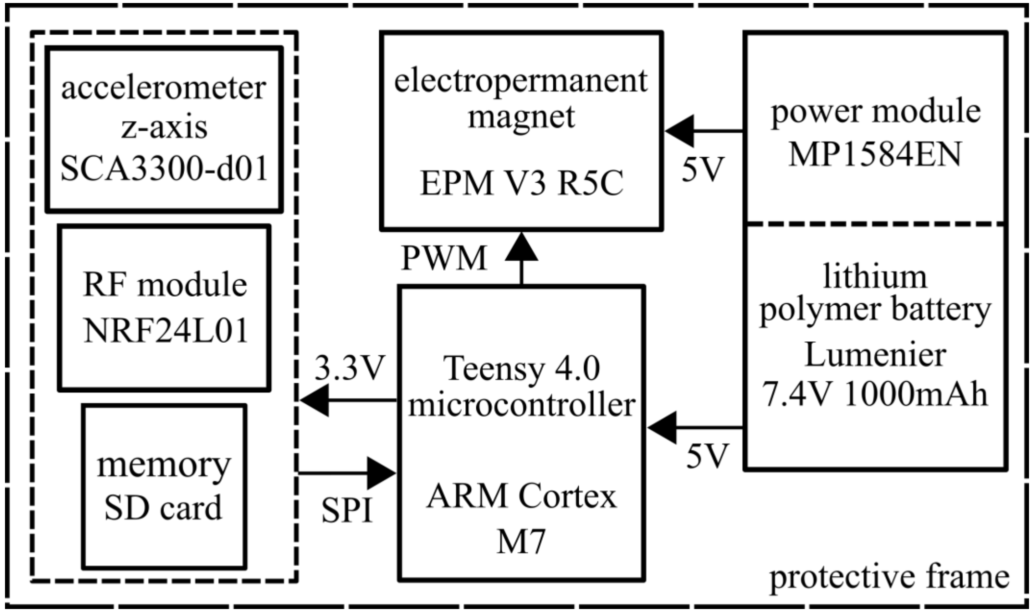

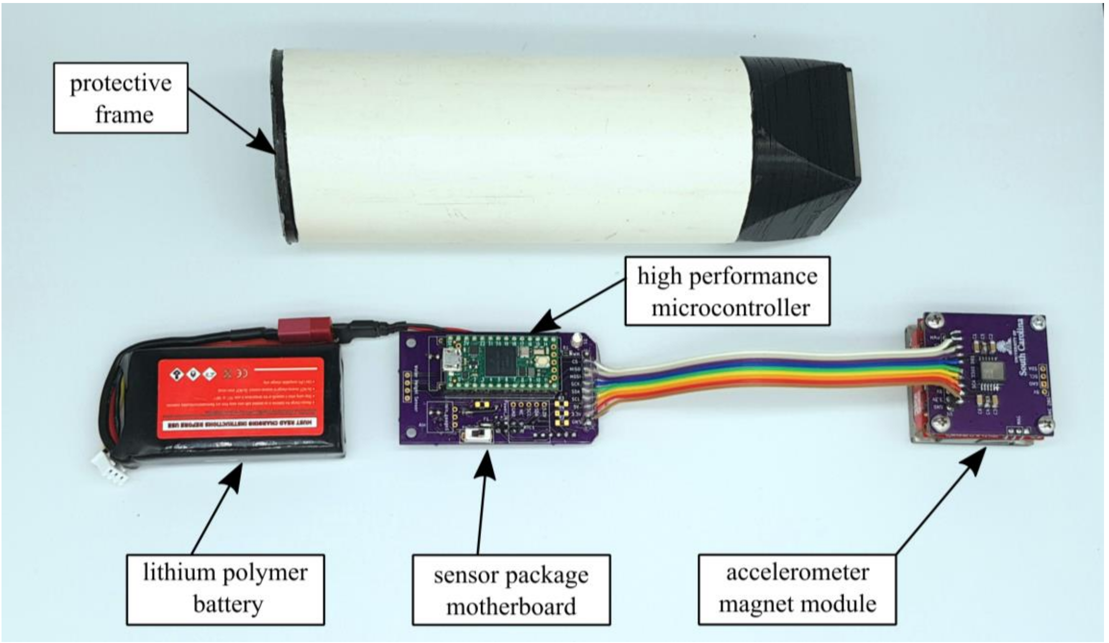

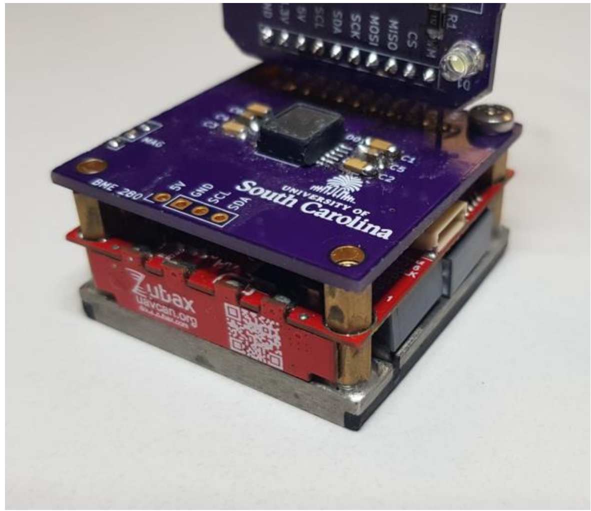

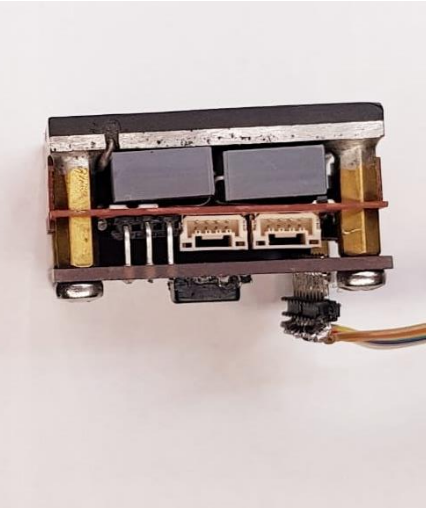

Sensor package breakdown

Developed on Arduino IDE and deployed on an ARM Cortex-M7 processor.

- Algorithm:
  - Initialize the magnet signaling start of deployment.
  - Acceleration data is periodically collected.
  - Data collected in a buffer to enable high sampling rates.
  - 74,000 timed samples are collected then transferred onto the memory.
  - Code initiates standby mode which turns modules off to converse power.
  - Microcontroller and wireless module remain on for communication.

- User interface:
  - A connection is achieved over 2.4 GHz ShockBurst protocol.
  - User can monitor operating conditions of the sensor package.
  - Retrieve stored data.
  - Issue commands to electropermanent magnet for retrieval.

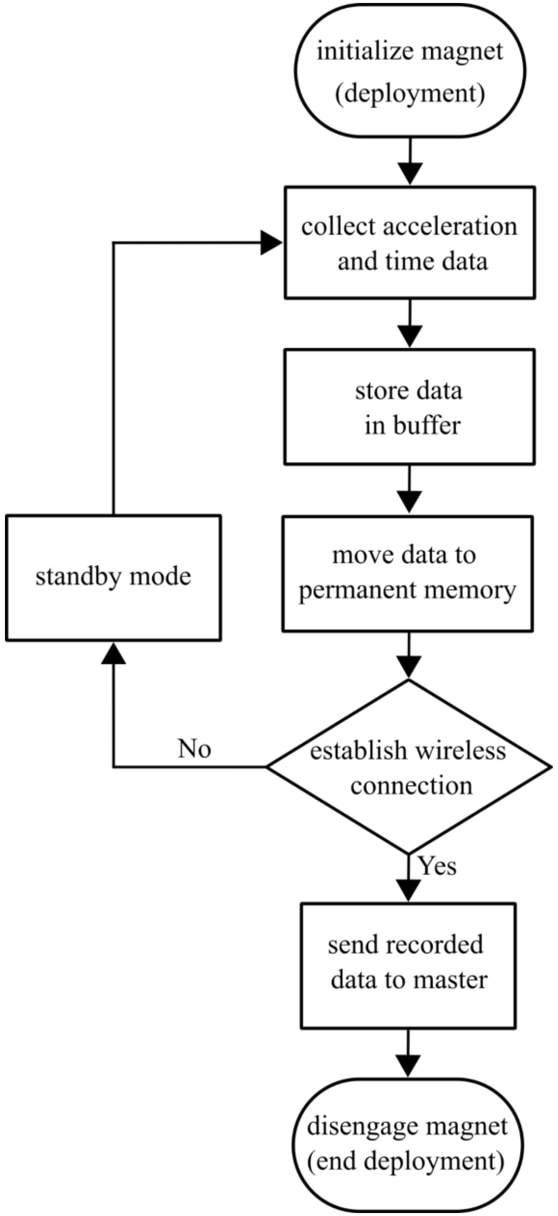

Deployment and retrieval

- Package is mounted onboard UAV.
- Contact is established with test structure.
- Electropermanent magnet on sensor package initiates.
- UAV electropermanent magnet disengages.
- Sensor package periodically collects data.
- UAV approaches structure and establishes contact with package.
- Electropermanent magnets toggle.
- UAV retrieves sensor package.

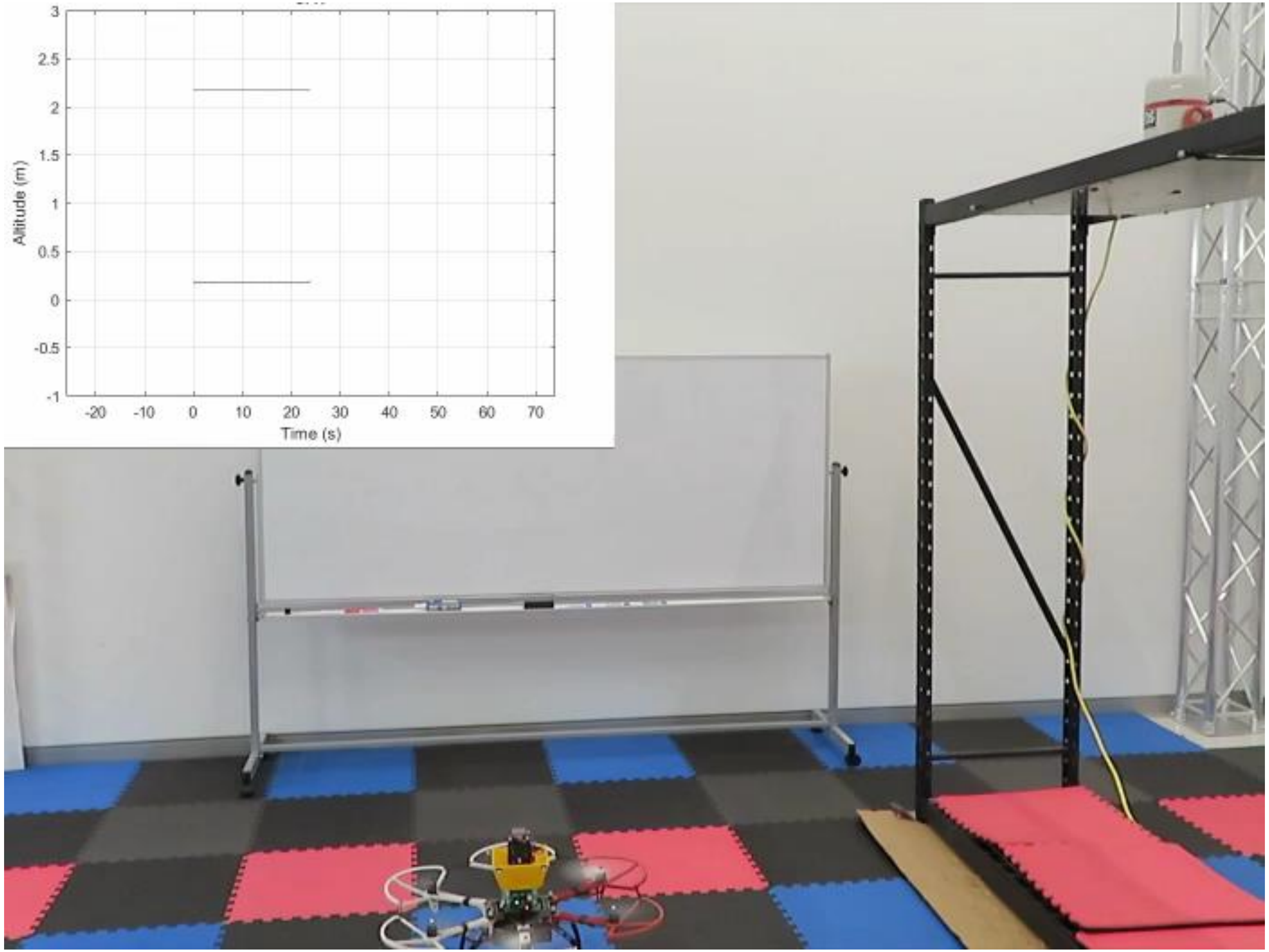

Transfer function-based filter

- Approach and assumptions:
  - Input-output relationship is acquired using frequency sweep excitation (Chirp).
  - A model of the physical sensor package ($Gp(s)$) is created.
  - Assumptions made about the plant $Gp(s)$:
    - Linearity
    - Causality
    - Minimal-phase system
  - $Gp(s)$ is inversed creating the filter $Gp^{-1}(s)$.
  - Using $Gp^{-1}(s)$, the influence of the plant is attenuated.
  - True acceleration obtained given only the output of $Gp(s)$.

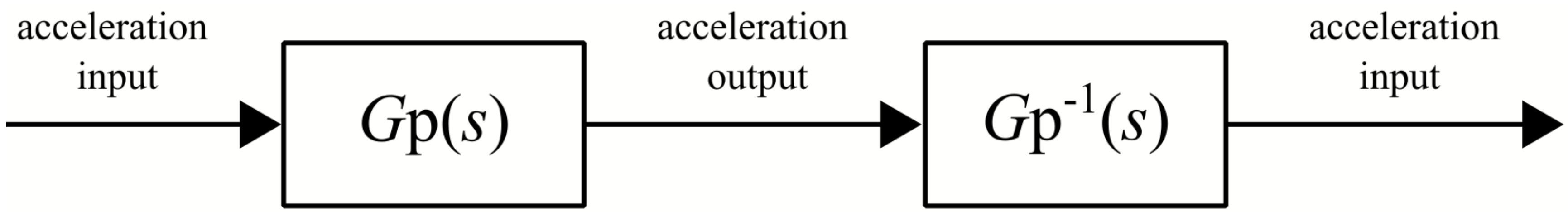

Transfer function-based filter

$$x(t) = \sin(1 + 2\pi(\frac{(f_1 - f_0)}{2T})t^2 + f_0 t)$$

- Model Training:
  - Using a chirp function:
    - $x(t)$ = frequency sweep function
    - $f_0 = 0.1$ Hz
    - $f_1 = 20.9$ Hz
  - $T = 40$ s
  - Excitation using electromagnetic shaker

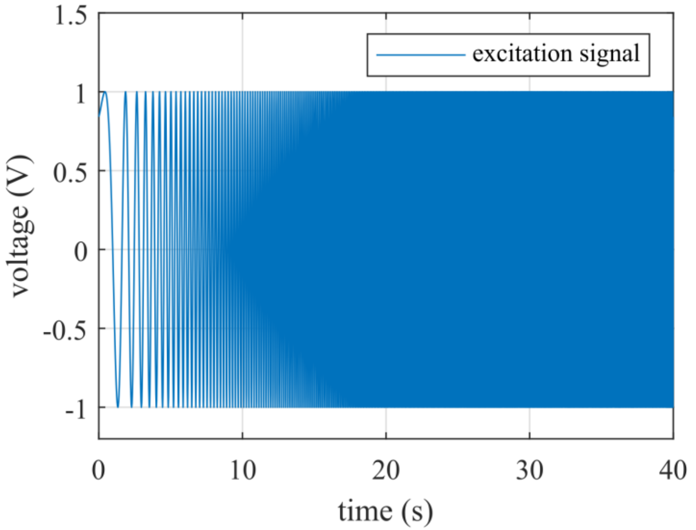

(a)

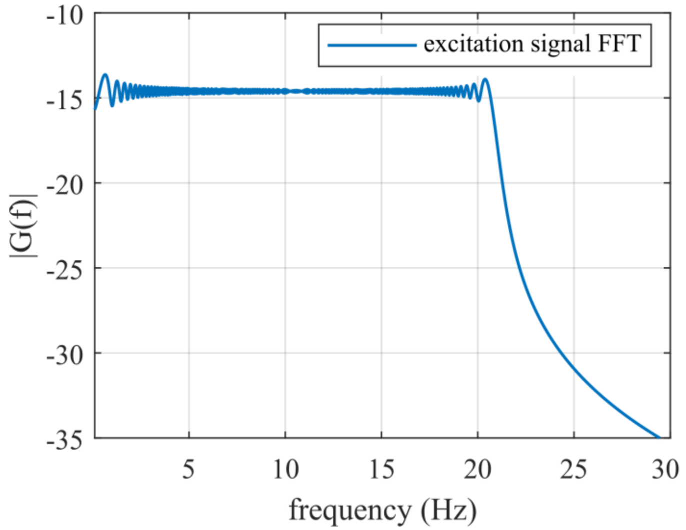

(b)

Bench-top testing (Training)

- Experimental parameters:
    - Bandwidth of interest: 0.1-20 Hz
    - Excitation source: Electromagnetic shaker
    - Reference accelerometer: Piezoelectric model 393B04
    - Sensor package hard-wired trigger.
    - Sampling rate: 1600 S/s

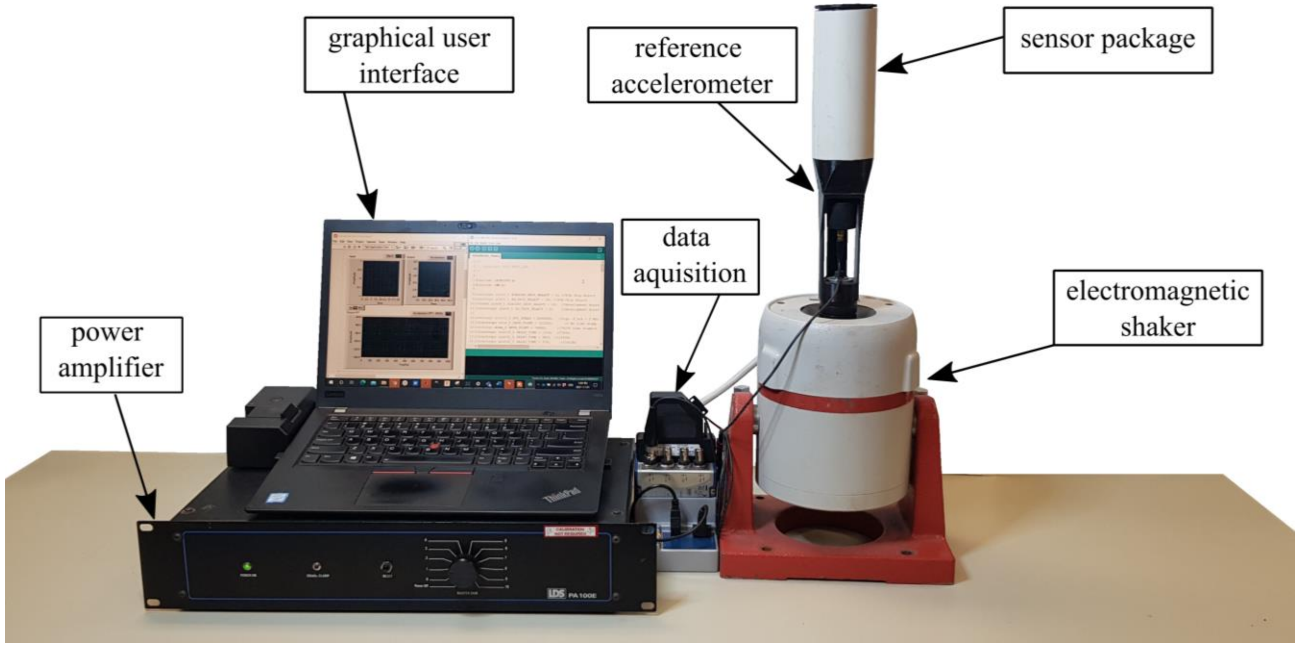

Bench-top testing (Training)

- Experimental procedure:
  - Synthesized Chirp voltage signal is fed into the shaker for excitation.
  - Reference accelerometer and sensor package are synchronized using a digital trigger
  - Through this experiment an input-output relationship is established.

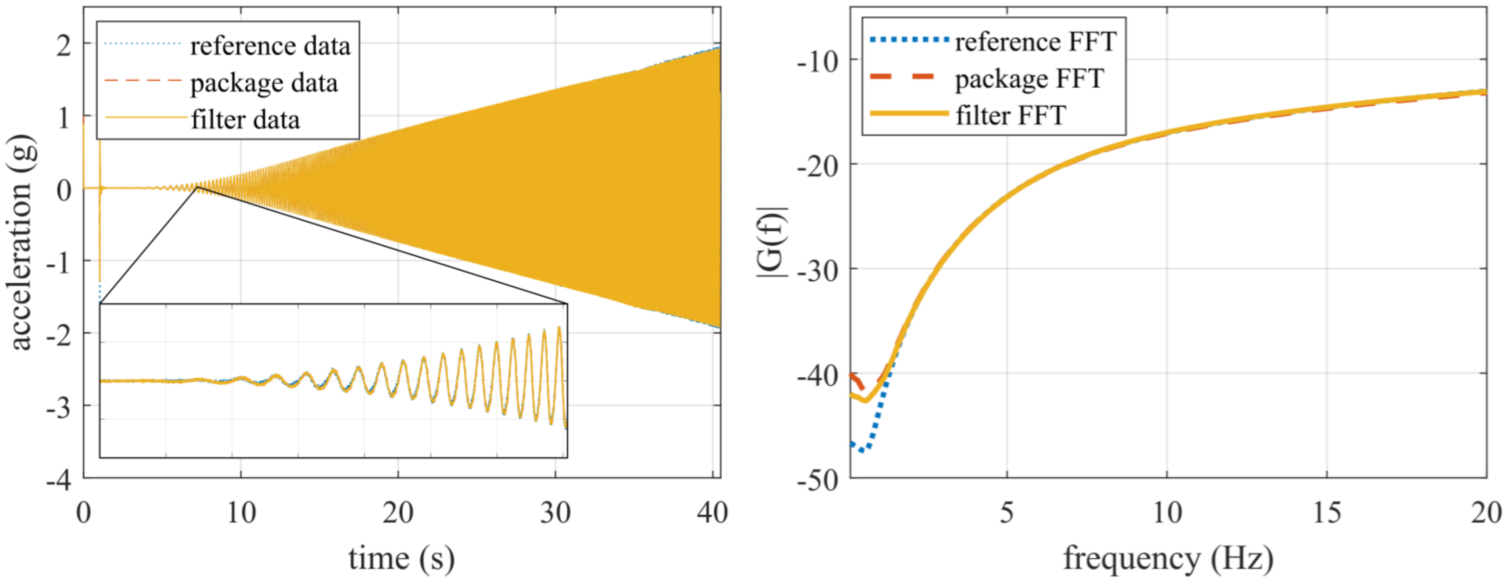

(a) (b)

Bench-top testing (Training)

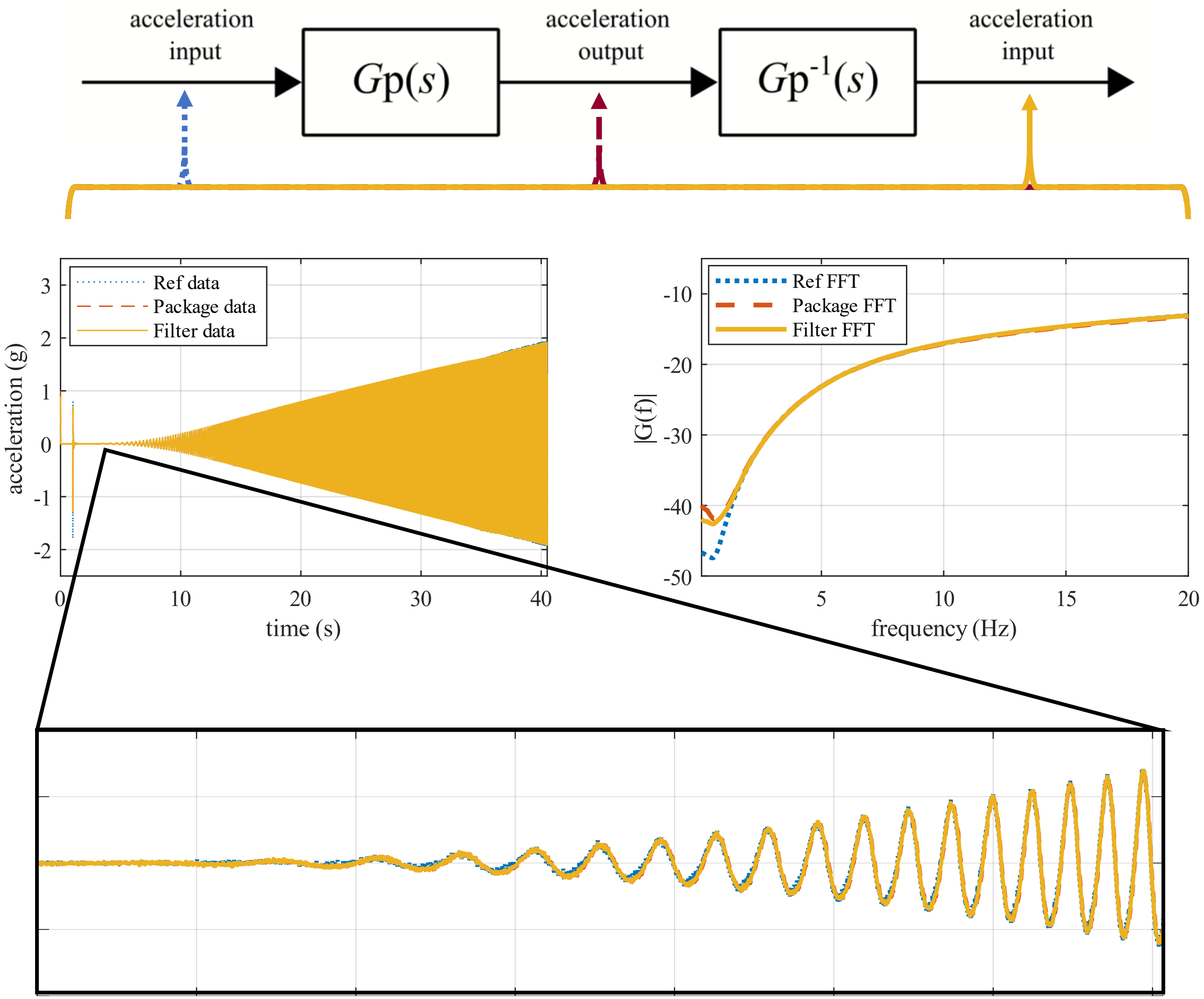

- Model training:
  - Multiple data sets are used in modeling.
  - Input: Reference accelerometer
  - Output: Sensor package
  - Transfer function model $Gp(s)$ is construc
  - Transfer function is then inversed creatin filter $Gp^{-1}(s)$.

Inverse plant transfer function:

$$Gp^{-1}(s) = \frac{s^3 + 668.8s^2 + 2.937 * 10^4 s + 3.58 * 10^4}{1.123s^3 + 652.1s^2 + 3.067 * 10^4 s + 7.393 * 10^4}$$

Structure test (Validation)

- Experimental parameters:
  - Steel test structure is constructed.
  - Data acquisition system:
    - Analog output generate excitation signal
    - Digital trigger to synchronize sensor package and reference accelerometer.
    - Data logging of reference acceleration.
  - Signal-to-noise ration was used to measure performance.

$$\mathrm{SNR_{dB}} = 10\log_{10}\left(\frac{\Sigma_{i=1}^{74000}(S(i))^2}{\Sigma_{i=1}^{74000}(N(i))^2}\right)$$

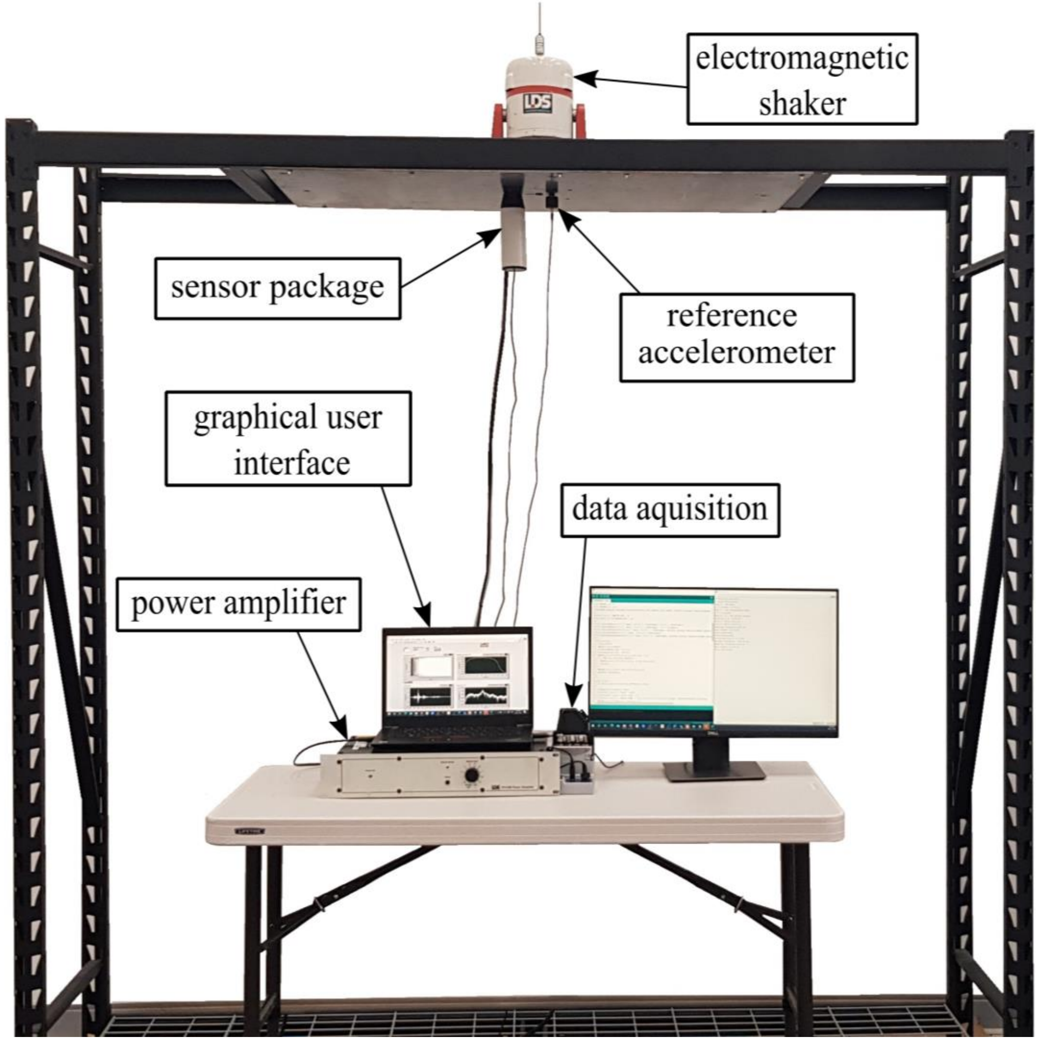

Structure test (Validation)

- Experimental procedure:
  - The sensor package is mounted onto test structure along with a reference accelerometer.
  - The electromagnetic shaker is secured on top as the source of excitation.
  - The package and reference accelerometers are triggered.
  - Chirp signal is routed to shaker through an amplifier.
  - Data sets are examined with and without filtering to gauge performance.

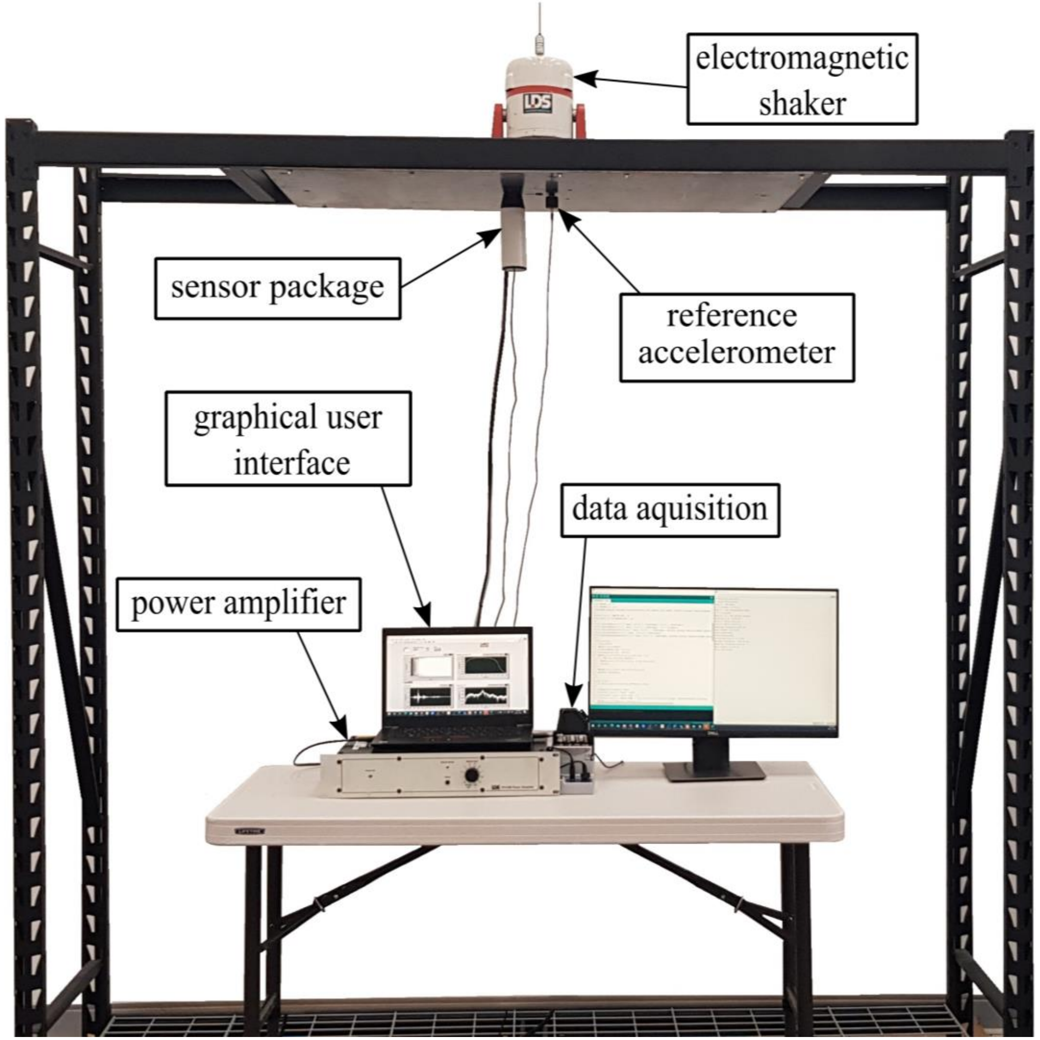

Experimental outcomes

- Structure test (Validation):
  - Filtered signal traces the reference with high correlation.
  - Frequency domain indicates enhancement in the range of 6-20 Hz.
  - Error percentage is considered negligible between 6-14 Hz (<0.4%).
  - Signal-to-noise ratio pre and post filtering is shown

Pre-filter SNR	16.74 dB	-
Post-filter SNR	17.94 dB	-
SNR increase	1.2 dB	7.17%

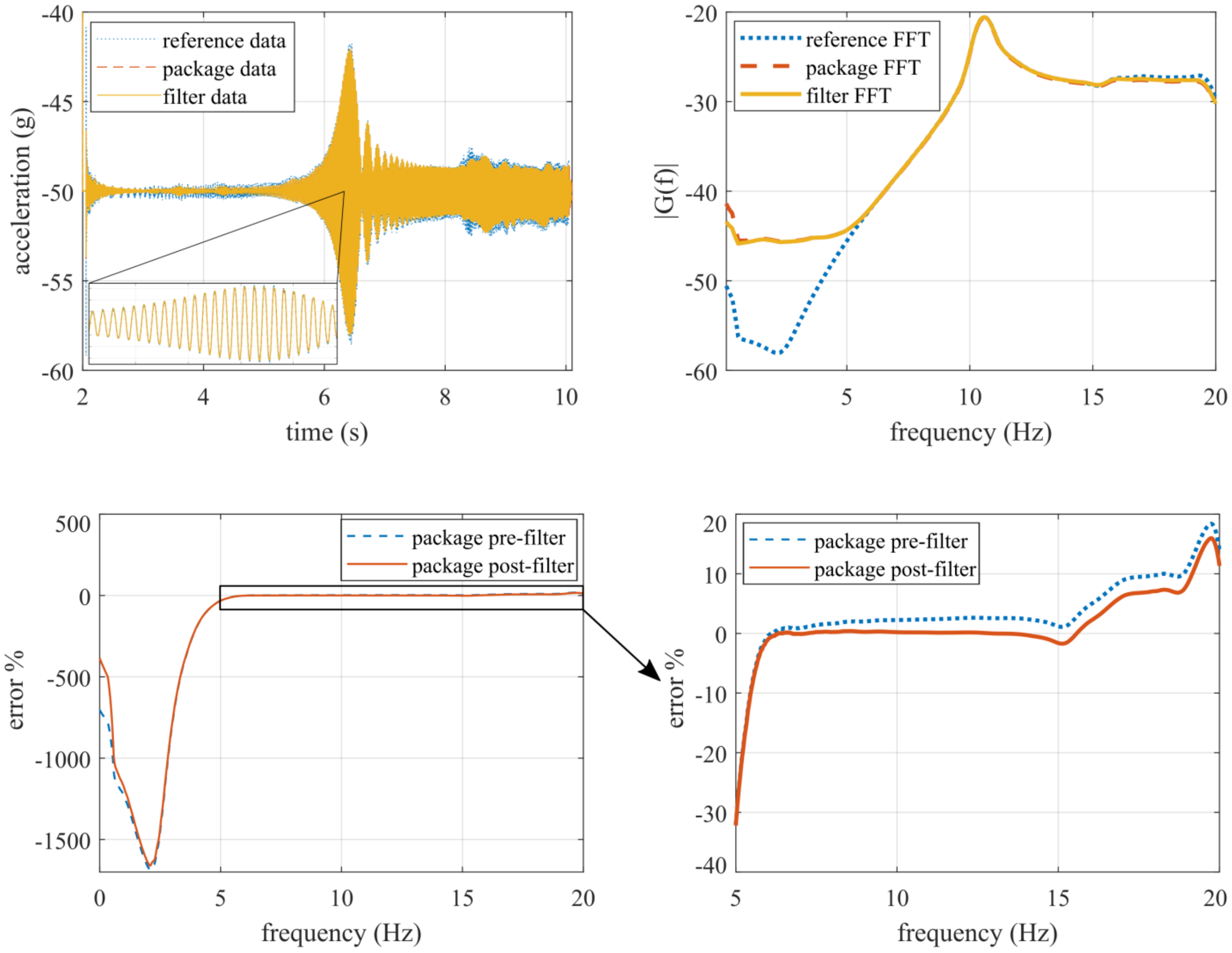

Structure test (Validation)

- Findings and limitations:
  - Diminishing returns of the filter can be observed in the range below 5 Hz.
  - Analog-to-digital converter (ADC) lack adequate resolution to detect the low-energy signal found in lower frequencies.

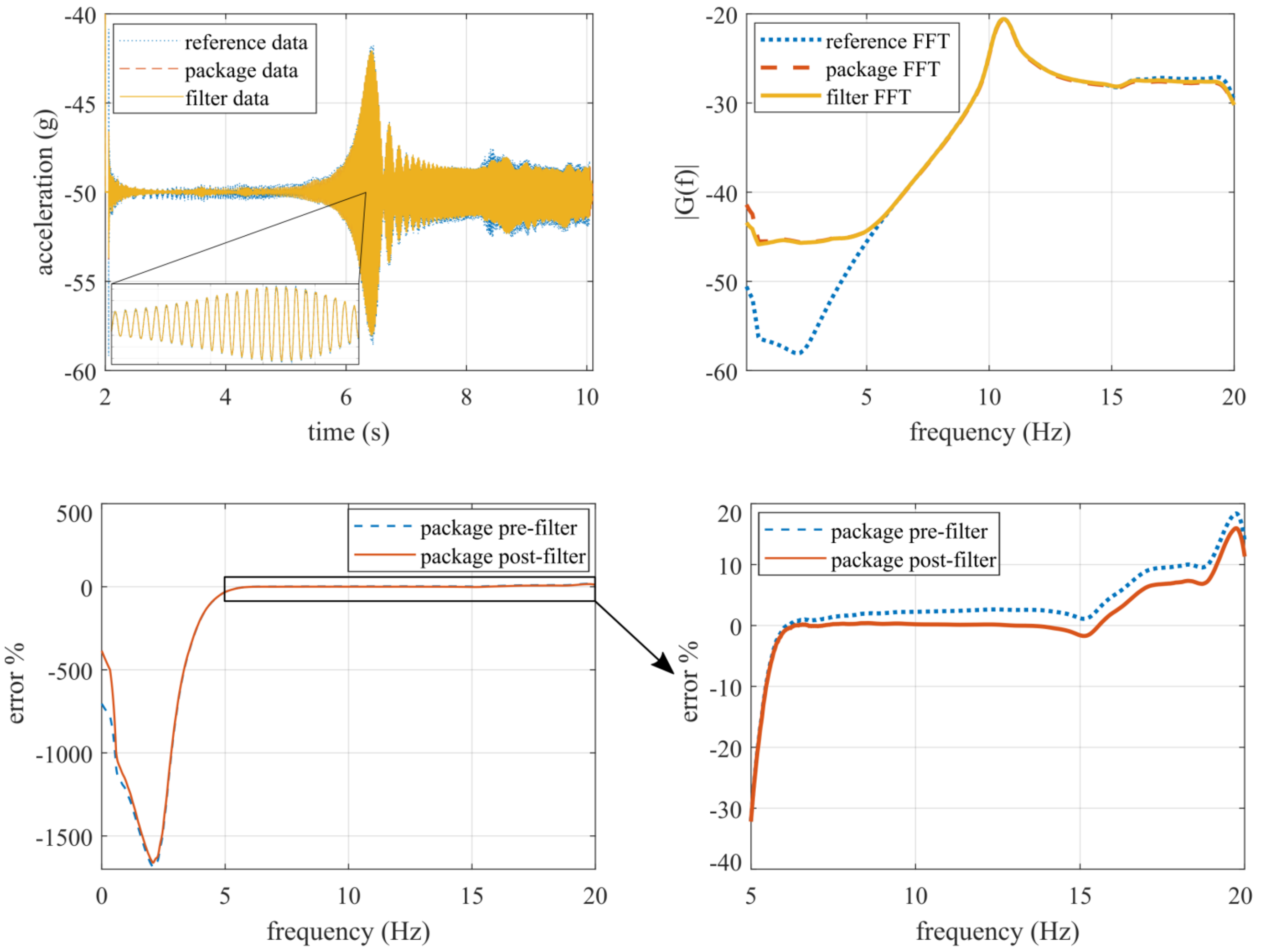

- **Future work**
  - Sensor improvement
    - Improve resolution of analog to digital converter onboard the sensor package.
    - Investigate sensor network deployment.
  - Edge implementation
    - Discretize transfer-function filter.
    - Investigate the feasibility of microcontroller implementation.

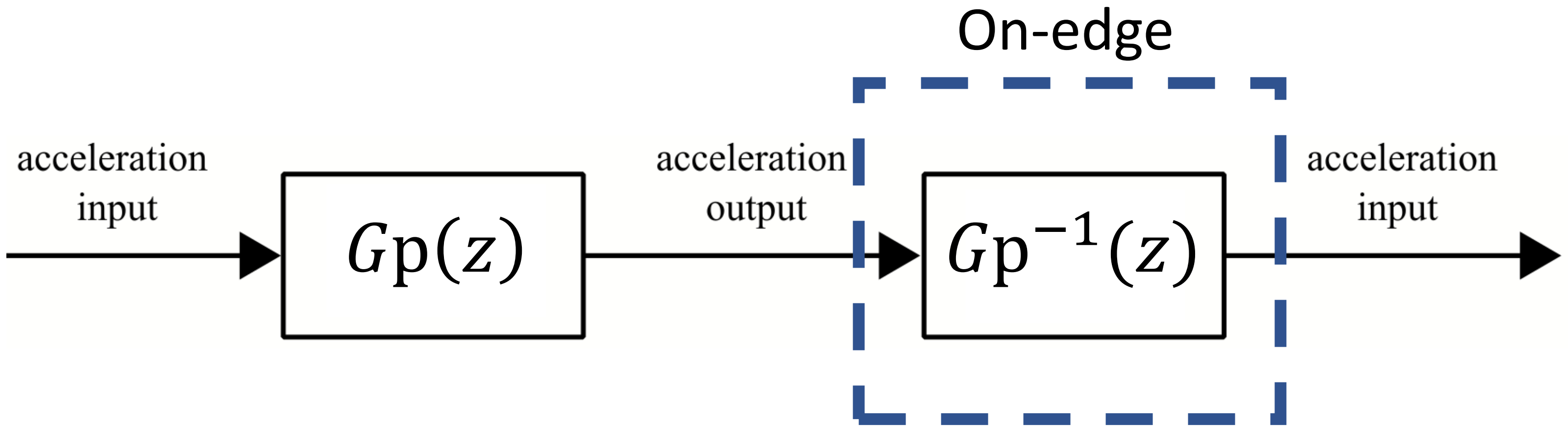

Thank you

Questions?

Contact Information
Name: Joud Satme
Email: Jsatme@email.sc.edu

References:

[1] Pakzad, S. N., Fenves, G. L., Kim, S., and Culler, D. E., “Design and implementation of scalable wireless sensor network for structural monitoring,” Journal of Infrastructure Systems 14, 89–101 (mar 2008).

[2] Sabato, A., Niezrecki, C., and Fortino, G., “Wireless mems-based accelerometer sensor boards for structural vibration monitoring: A review,” IEEE Sensors Journal 17(2), 226–235 (2017).

[3] Carroll, S., Satme, J., Alkharusi, S., Vitzilaios, N., Downey, A., and Rizos, D., “Drone-based vibration monitoring and assessment of structures,” Applied Sciences 11(18) (2021).

[4] Takeuchi, K., Masuda, A., Akahori, S., Higashi, Y., and Miura, N., “A close inspection and vibration sensing aerial robot for steel structures with an EPM-based landing device,” in [Nondestructive Characterization and Monitoring of Advanced Materials, Aerospace, and Civil Infrastructure 2017], Wu, H. F., Gyekenyesi, A. L., Shull, P. J., and Yu, T.-Y., eds., 10169, 666 – 677, International Society for Optics and Photonics, SPIE (2017).

[5] Chen, B. and Liu, W., “Mobile agent computing paradigm for building a flexible structural health monitoring sensor network,” Computer-Aided Civil and Infrastructure Engineering 25, 504–516 (aug 2010).

[6] Badri, A. E., Sinha, J. K., and Albarbar, A., “A typical filter design to improve the measured signals from mems accelerometer,” Measurement 43(10), 1425–1430 (2010).

[7] Karpel, M. and Ricci, S., “Experimental modal analysis of large structures by substructuring,” Mechanical Systems and Signal Processing 11(2), 245–256 (1997).

[8] Sim, S.-H., Li, J., Jo, H., Park, J.-W., Cho, S., Jr, B. F. S., and Jung, H.-J., “A wireless smart sensor network for automated monitoring of cable tension,” Smart Materials and Structures 23, 025006 (dec 2013).

[9] Ubertini, F., Comanducci, G., and Cavalagli, N., “Vibration-based structural health monitoring of a historic bell-tower using output-only measurements and multivariate statistical analysis,” Structural Health Monitoring 15(4), 438–457 (2016).

[10] Johnson, D. H., “Signal-to-noise ratio,” Scholarpedia 1(12), 2088 (2006). revision #126771.

[11] Ljung, L., System Identification Toolbox (2014)